Colloid Polym Sci (2008) 286:1093–1096
DOI 10.1007/s00396-008-1865-3

SHORT COMMUNICATION

Porous carbon and carbon composite hollow spheres

Shujiang Ding · Chengliang Zhang · Xiaozhong Qu · Jiguang Liu · Yunfeng Lu · Zhenzhong Yang

Received: 12 October 2007 / Revised: 22 December 2007 / Accepted: 7 March 2008 / Published online: 30 May 2008

Abstract In this communication, we propose a template approach toward synthesis of carbon hollow spheres by direct carbonization of highly crosslinked sulfonated polystyrene gel hollow spheres (sPS). The sulfonic acid group can facilitate carbonization. Moreover, the acid group can also induce a favorable growth of other materials within the sPS gel-forming carbon-based composite shell such as bicontinuous C/SiO_2 and their derivative ceramic SiC. Release of small molecules during polymers decomposition results porous shell.

Keywords Carbon · Composite · Hollow spheres

Introduction

Hollow spheres and capsules have spurred great interest due to their broad applications [1–7]. Among these materials, hollow carbon spheres with shorter transportation pathway than their counterpart solid ones are in particular promising owning to their potential applications, such as catalyst supports [8] and anode materials in lithium secondary batteries [9]. Generally, hollow carbon spheres are synthesized by shock-compression technique [10], pyrolysis of a core-shell latex [11], solvothermal synthesis [12–14] which require rigorous conditions, expensive apparatus, or lack of structural control. It is, therefore, desired to develop a facile and scaleable method enabling the efficient synthesis of hollow carbon spheres.

Recently, some novel methods have been developed for facile synthesis of mesoporous carbon hollow spheres such as by chemical vapor deposition or pyrolysis of polymer against mesoporous inorganic templates.[15–17] Both particle size and microstructure of the shell can be tuned. However, the shell may be easily fractured by the arisen osmotic pressure during the template removal. However, it is not easy to incorporate other functional materials within the carbon matrix especially in one step.

The synthesis of hollow carbon and carbon nanocomposite spheres. As schematically illustrated in Scheme 1, our synthesis strategy begins with sulfonated hollow polystyrene spheres (sPS). Carbonization process catalyzed by the embedded sulfuric acid moiety ($-SO_3H$) [18–20] converts the spheres into hollow carbon spheres. Small molecules released during this process create pores within the carbon shells and form a porous network. Meanwhile, various building components, such as metal ions and clusters of metal oxide, can be readily absorbed or grown within the sPS shells [21–24], which provides a simple and flexible approach to synthesize various carbon nanocomposite spheres in one step. As a proof of the concept, a sol–gel process of silica can be undertaken within the sPS shells to form hollow silica or sPS spheres. Carbonization and subsequent high temperature treatment convert the silica or sPS spheres into hollow carbon or silica nanocomposite spheres and crystalline SiC spheres, respectively. Different from the conventional core-shell based synthesis, the step

Electronic supplementary material The online version of this article (doi:10.1007/s00396-008-1865-3) contains supplementary material, which is available to authorized users.

S. Ding · C. Zhang · X. Qu · J. Liu · Y. Lu · Z. Yang (✉)
State Key Laboratory of Polymer Physics and Chemistry,
Institute of Chemistry, Chinese Academy of Sciences,
Beijing 100080, China
e-mail: yangzz@iccas.ac.cn

Y. Lu (✉)
Department of Chemical and Biomolecular Engineering,
University of California at Los Angeles,
Los Angeles, CA 90095-1592, USA
e-mail: luucla@ucla.edu

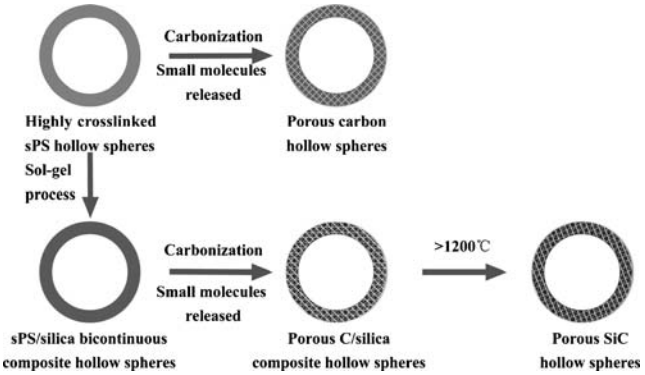

Scheme 1 Schematic of the synthesis of hollow carbon and carbon composite spheres

of removing the core templates is avoided in this synthesis scheme, providing a more efficient and simple method to prepare hollow carbon and carbon nanocomposite spheres with well-controlled spherical morphology. Due to the hierarchical porous structure, both the performances of enhanced mass transportation through the big cavity and high absorption capacity from the micro- and mesoporous shell are integrated. Besides, the thermal stability in air of carbon is highly improved after the incorporation of inorganic materials. This is urgently required in many application areas such as catalysts supporting for fuel cells.

Results and discussion

The carbonization process was investigated by thermal gravimetric analysis (TGA) as shown in Fig. 1. As known, the decomposition of linear polystyrene begins at 370 °C and is completed at 450 °C (see Fig. S1). In comparison, the sPS spheres experience a two-stage decomposition at 200–300 °C and 300–400 °C (trace a), which corresponds to the formation of sulfone bridge (R–SO_2–R, where R is an aromatic ring) through dehydration of the sulfonic acid group (-SO_3H), and the further sulfur bridging (R–S–R) through deoxidation reaction, respectively. [19] These newly formed bridging bonds provide extra crosslinking structure and enhance their thermal stability, resulting in 15 wt.% of carbon yield after carbonization at 800 °C. Therefore, a pretreatment at 370 °C for 2 h prior to the carbonization was used to improve the carbon yield. As a result, the pretreated spheres exhibit a higher carbon yield of 21 wt.% (trace b). However, it was found that the carbonized samples contained a large faction of broken spheres. To retain the spherical contour, we further enforce the polymer sphere structure by crosslinking the polystyrene spheres through copolymerizing styrene and divinylbenzene (DVB). Subsequent sulfonating process creates more robust polymer spheres and led to the successful synthesis of hollow carbon spheres with well-controlled spherical contour. It was also found that a much higher carbon content of 39 wt.% (trace c) was obtained.

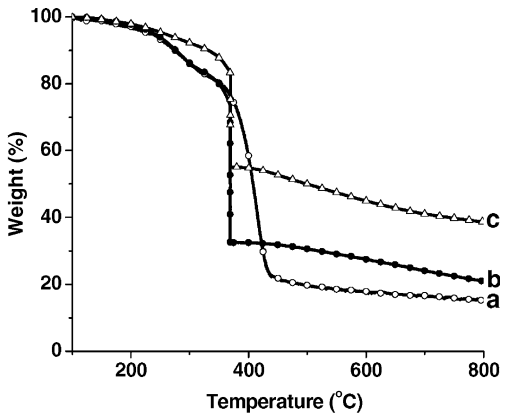

Fig. 1 TGA traces of *a* (*empty circles*) the sulfonated linear polystyrene spheres before and *b* (*filled circles*) after pre-treatment at 370 °C for 2 h and *c* (*empty triangles*) the sulfonated crosslinked polystyrene hollow spheres after pretreatment at 370 °C for 2 h

Crosslinked polystyrene hollow spheres composed of linear polystyrene and crosslinked St–DVB are a semi-interpenetrating polymer network structure. Figure 2a shows scanning electron microscopic and transmission electron microscopic (TEM) images of the crosslinked polystyrene spheres with a mean shell thickness of 80 nm and cavity diameter of 320 nm. The spherical morphology is retained after being sulfonated (Fig. 2b), and the shell thickness was increased to 120 nm and the cavity diameter was decreased to 280 nm. Such sulfonated spheres (S1) provide robust templates for the synthesis of hollow carbon spheres. Figure 2c shows a TEM image of the resulted carbon spheres, indicating a shell thickness of 100 nm and cavity diameter of 200 nm. Carbon hollow spheres can well retain shell structure. Raman (Fig. S2), X-ray diffraction (XRD; Fig. S3), and high resolution TEM (HR-TEM) image (Fig. 2d) indicate that the carbon shell is amorphous

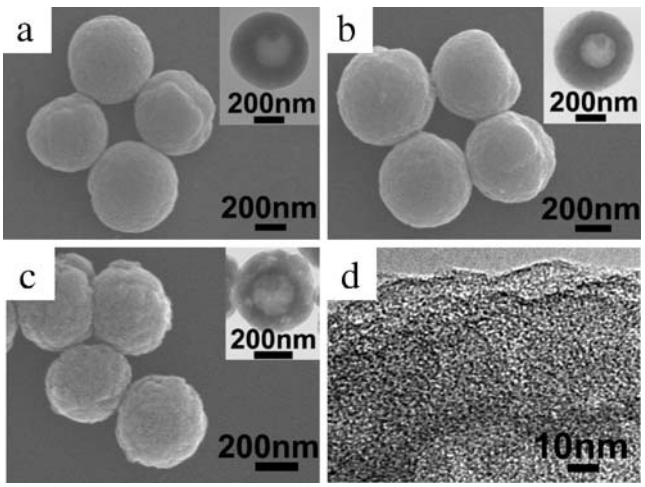

Fig. 2 SEM and TEM (*inset*) image of the crosslinked polystyrene hollow spheres S1 **a** before sulfonation, **b** after sulfonation; **c** after carbonization, and HRTEM image of the carbon sphere shell (**d**)

[25] containing worm-like pore channels. Typical hysteretic-type H4 [26] nitrogen sorption isotherms indicate the presence of micropores and mesopores (Trace I, Fig. S4). The BET surface area is around 637 m^2g^{-1}; t-plot specific surface area contributed by the micropore is 531 m^2g^{-1}. The total pore volume is 0.40 cm^3g^{-1}, to which the micropore contributes 0.24 cm^3g^{-1}. The mesopore size is around 4.2 nm, and the micropore size calculated by Horvath–Kawazoe adsorption method (slit pore geometry) is around 0.46 nm. The presence of such multi-length-scale pore structure (e.g., hollow cavities, micropores, and mesoporous pores) is of great interest because the hollow cavities may provide fast mass transport pathways while the micropores and mesopores can provide high surface areas, selectivity, and adsorption capability. [27, 28]

The sulfonic acid group ($-SO_3H$) can adsorb metal ions and other inorganic species within the spheres, allowing efficient synthesis of carbon composites spheres. For example, Fig. 3a shows a TEM image of S1–Pd composite spheres, which was prepared by adsorbing palladium ions within the sulfonated spheres and subsequent reducing reaction. The cross-sectional TEM image demonstrates that Pd nanoparticles with a mean particle size 10 nm are favorably distributed within the whole shell. Carbonizing these spheres produced carbon–Pd composite spheres (Fig. 3b). The Pd nanoparticles exhibit the face-centered cubic structure confirmed by XRD (Fig. S3) [29, 30] and HR-TEM image (inset Fig. 3b, {111} crystalline lattice 0.225 nm). Note that the particle size was increased from 10 to 20–30 nm after carbonization.

This method can be generalized to synthesis a class of carbon–ceramic composite hollow spheres. Using the synthesis of carbon–silica as an example, we incorporated silicate species within the sulfonated spheres by mixing tetraethoxysilane (TEOS) with the spheres S1 in water–ethanol. The sulfonic acid group catalyzes the hydrolysis and condensation reactions of TEOS, resulting in the formation of S1–silica composite spheres. Note that excess silicate species can also diffuse thorough the polymer shell layer, creating a silica particle within the cavity (see Fig. 3c). This formation process is similar to the template synthesis of nanoparticles inside the cavity of virus templates. [31] Subsequent carbonization process converts the S1–silica spheres into carbon–silica composite hollow spheres (Fig. 3d). To investigate the structure of the composite spheres, we selectively removed silica or carbon from the composite spheres using hydrofluoric acid etching or calcination method, respectively. TEM images of the resulted carbon and silica spheres are shown in Fig. 3e and f, respectively. The well-retained spherical shape indicates silica–carbon composite shells contain a bicontinuous structure.

BET specific surface area of the silica–carbon composite spheres is around 325 m^2g^{-1} while the t-plot micropore surface area is around 249 m^2g^{-1}. The micropore diameter is 0.47 nm, and the mesopore diameter is 3.85 nm (trace II, Fig. S4). After the dissolution of silica, the carbon spheres show a typical hysteretic H3 sorption isotherms with an increased BET specific surface area (493 m^2g^{-1}) and decreased t-plot micropore surface area (103 m^2g^{-1}). The mean diameter of the mesopores and micropores is around 4.4 and 0.47 nm, respectively (trace III, Fig. S4). Similarly, removal of the carbon resulted in hollow porous silica spheres with BET-specific surface area of 349 m^2g^{-1} and t-plot micropore surface area of 38 m^2g^{-1} (trace IV, Fig. S4).

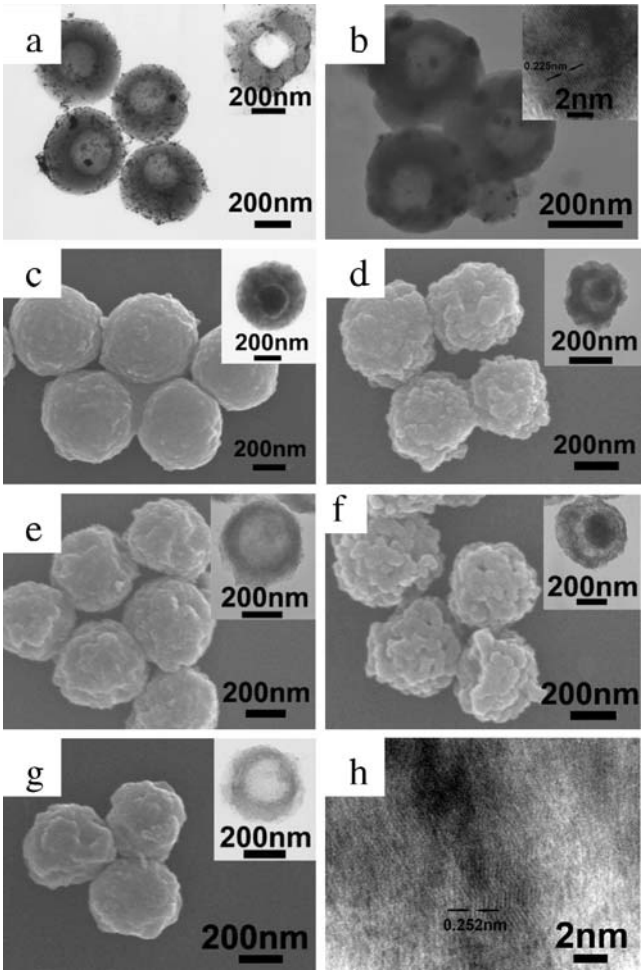

Fig. 3 Morphologies of the composite hollow spheres. **a** TEM images of S1–Pd composite hollow spheres; **b** TEM image of carbon–Pd composite hollow spheres and HR-TEM image (*inset*) of a Pd nanoparticle; **c** SEM and TEM (*inset*) images of the S1–silica composite spheres; **d** SEM and TEM (*inset*) images of the carbon–silica composite hollow spheres; **e** SEM and TEM (*inset*) images of the carbon hollow spheres prepared by removing silica from the carbon–silica composite spheres; **f** SEM and TEM (*inset*) images of the silica spheres prepared by removing carbon from the carbon–silica composite spheres; **g** SEM and TEM (*inset*) images of SiC spheres; **h** HR-TEM image of the SiC hollow spheres

Compared with silica–carbon nanocomposites, SiC often shows better thermal stability, chemical stability, and other excellent properties. We, therefore, converted the carbon–

silica composite spheres to hollow SiC spheres at high temperature (e.g., 1,300 °C) under argon. Dark green SiC hollow spheres with well-preserved spherical contour were achieved (Fig. 3g). XRD result reveals a β-SiC (trace d, Fig. S3) and their {111} crystalline lattice (0.252 nm) is also shown by HR-TEM study (Fig. 3h). More importantly, nitrogen adsorption–desorption isotherms show a typical hysteresis H3, indicating that SiC shell is mesoporous with an averaged pore size diameter of 3.9 nm and BET area of 598 m^2g^{-1} (Fig. S5). Such highly stable mesoporous SiC hollow spheres are of great interest for high temperature catalyst support and many other applications [32].

Conclusions

We have demonstrated a novel approach to synthesize hollow carbon and carbon composite spheres. Such spheres contain hierarchical pore structure within their shells, providing enhanced mass transfer and higher absorption capacity for many applications. The approach can be generalized to prepare a large family of composite hollow spheres with designed functionality and tailored pore structure for a large spectrum of applications.

Acknowledgments This work was supported by National Science Foundation of China (50573083, 50325313, 90606031 and 50521302), foundations from Chinese Academy of Sciences, and China Ministry of Science and Technology (2004-01-09, KJCX2-SW-H07 and 2003CB615600).

Supporting Information Sample preparation and characterization, Raman spectrum, TGA curve, Nitrogen adsorption–desorption isotherms, and Fourier transform infrared spectra of sample.

References

1. Caruso F (2000) Chem Eur J 6:413
2. Caruso F (2001) Adv Mater 13:11
3. Caruso F, Caruso RA, Möhwald H (1998) Science 282:1111
4. Donath E, Sukhorukov GB, Caruso F, Davis SA, Möhwald H (1998) Angew Chem Int Ed 37:2202
5. Sukhorukov GB, Donath E, Lichtenfeld H, Knippel E, Knippel MA, Möhwald H (1998) Colloids Surf A 137:253
6. Wilcox DL, Berg M, Bernat T, Kelleman D, Cochran JK (1995) Hollow and Solid Spheres and Microspheres: Science and Technology Associated with their Fabrication and Applications, Materials Research Society Proceedings, vol. 372. MRS, Pittsburgh
7. Zhong ZY, Yin YD, Gates B, Xia YN (2000) Adv Mater 12:206
8. Chai GS, Yoon SB, Kim JH, Yu JS (2004) Chem Commun 23:2766
9. Lee KT, Jung YS, Oh SM (2003) J Am Chem Soc 125:5652
10. Niwase K, Homae T, Nakamura KG, Kondo K (2002) Chem Phys Lett 362:47
11. Tamai H, Sumi T, Yasuda H (1996) J Colloid Interface Sci 177:325
12. Xiong YJ, Xie Y, Li ZQ, Wu CZ, Zhang R (2003) Chem Commun 7:904
13. Liu JW, Shao MW, Tang Q, Chen XY, Liu ZP, Qian YT (2002) Carbon 411:1682
14. Shen JM, Li JY, Chen Q, Luo T, Yu WC, Qian YT (2006) Carbon 44:190
15. Xia YD, Mokaya R (2004) Adv Mater 16:886
16. Yoon SB, Sohn K, kim JY, Shin CH, Yu JS, Hyeon T (2004) Adv Mater 14:19
17. Li YS, Yang YQ, Shi JL, Ruan ML Micropor Mesopor Mater (2007), DOI 10.1016/j.micromeso.2007.10.042
18. Yoon SB, Kim JY, Yu JS (2001) Chem Commun 6:559
19. Matsuda M, Funabashi KJ (1987) Polym Sci Part A: Polym Chem 25:669
20. Mbileni CN, Prinsloo FF, Witcomb MJ, Coville NJ (2006) Carbon 44:1476
21. Yang ZZ, Niu ZW, Lu YF, Hu ZB, Han CC (2003) Angew Chem Int Ed 42:1943
22. Niu ZW, Yang ZZ, Hu ZB, Lu YF, Han CC (2003) Adv Funct Mater 13:949
23. Yang M, Ma J, Niu ZW, Xu HF, Meng ZK, Lu YF, Hu ZB, Yang ZZ (2005) Adv Funct Mater 15:1523
24. Yang M, Ma J, Zhang CL, Lu YF, Yang ZZ (2005) Angew Chem Int Ed 44:6727
25. Yang XG, Li C, Wang W, Yang BJ, Zhang SY, Qian YT (2004) Chem Commun 3:342, 343
26. Gregg SJ, Sing KS (1982) Adsorption surface area and porosity, 2nd edn. Academic, New York
27. Anderson MW, Holmes SM, Hanif N, Cundy CS (2000) Angew Chem Int Ed 39:2707
28. Brandhuber D, Huesing N, Raab CK, Torma V, Peterlik H (2005) J Mater Chem 15:1801
29. Kim SW, Park J, Jang Y, Chung Y, Hwang S, Hyeon T (2003) Nano Lett 3:1289
30. Mandal S, Roy D, Chaudhari RV, Sastry M (2004) Chem Mater 16:3714
31. Meldrum FC, Wade VJ, Nimmo DL, Heywood BR, Mann S (1991) Nature 349:684
32. Liu RL, Shi YF, Wan Y, Meng Y, Zhang FQ, Gu D, Chen ZX, Tu B, Zhao DY (2006) J Am Chem Soc 128:11652